Supporting Information

Hochberg et al. 10.1073/pnas.1322673111

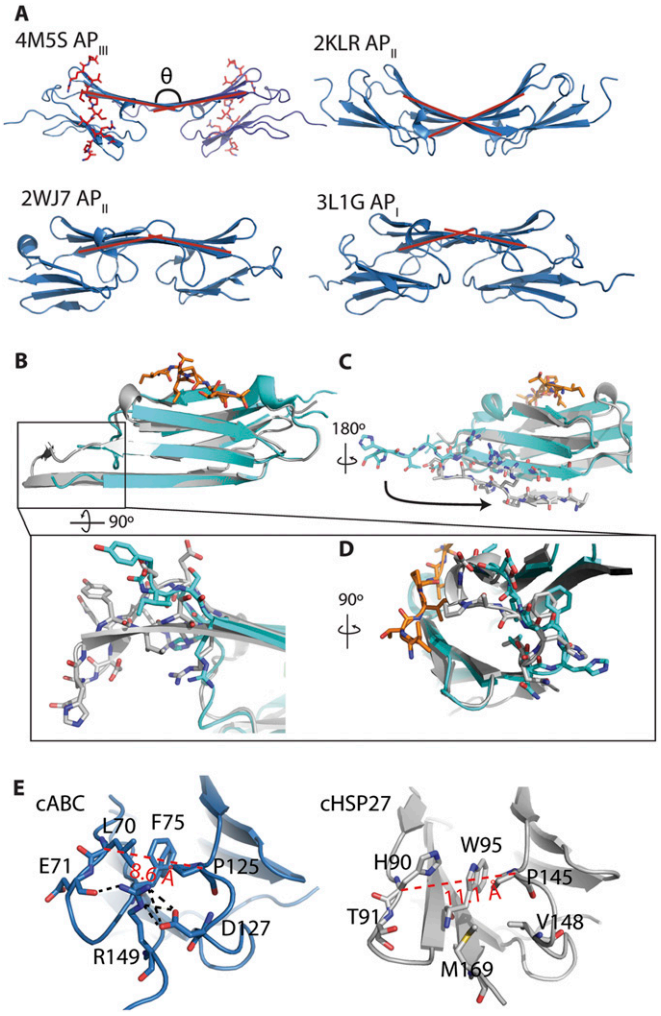

Fig. S1. (*A*) Comparison of X-ray and solid-state NMR structures of small heat-shock protein (sHSP) α-crystallin domain (ACD) structures. The solid-state NMR structure of αB-crystallin (ABC) [Protein Data Bank (PDB) ID code: 2KLR] has a bent dimer interface, which is partly mirrored in our AP_{III} structure [Research Collaboratory for Structural Bioinformatics (RCSB) PDB ID: 4M5S]. AP_{II} (PDB ID code: 2WJ7) and AP_{I} (PDB ID code: 3L1G) crystal structures show flatter dimer interfaces. Red lines indicate the angle θ between the two β-strands forming the dimer interface. (*B*) Overlay of our cHSP27 structure (RCSB PDB ID 4MJH, gray) and peptide in orange with a previous structure that crystallized as a crystallographic hexamer (PDB ID code: 3Q9P, cyan). *Inset* shows the region around the β5–β6+7 loop that is ordered in our structure by a longer β6+7 β-strand that forms part of the dimer interface. (*C*) The longer N terminus in our construct allows formation of the β2 strand. (*D*) Differences in the β3–β4 loop between our structure and 3Q9P. (*E*) Repacking in the β-sandwich in cHSP27 compared with cABC. In aligning cABC to cHSP27, we find that F75 is replaced by the bulkier W95, L70 by H90, which disrupts van der Waals interactions in the core, and R149 by M169, which abolishes salt-bridges to both sides of the β-sandwich (specifically to D127 and carbonyl of E71).

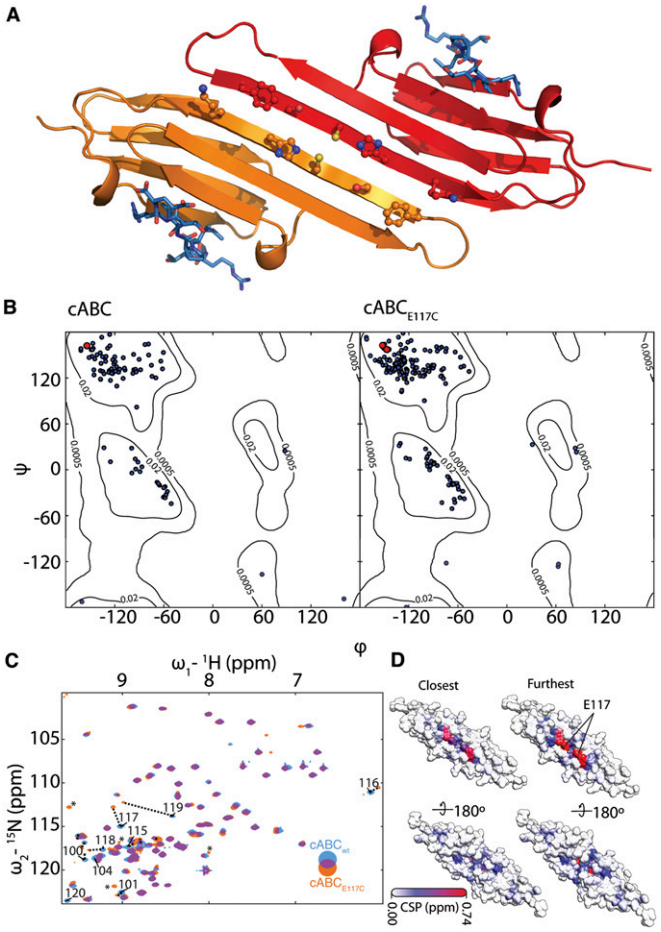

Fig. S2. (*A*) Second dimer in the asymmetric unit of the core domain of ABC (cABC$_{E117C}$), with the disulfide bond absent, likely as a consequence of radiation damage during data collection (1). The loop between β5 and β6+7 is ordered in this dimer. (*B*) C117 is not strained in cABC$_{E117C}$. Ramachandran plots for cABC (*Left*) and cABC$_{E117C}$ (*Right*). Red dots correspond to residue 117, which has normal β-sheet φ and ψ angles. Numbers on contour lines correspond to probabilities. The χ1 (65.37), χ2 (−33.22), χ3 (70.76), χ2′ (−44.41), and χ1′ (58.45) dihedral angles along the disulfide bond are within the range of unstrained cysteines. (*C*) A small number of resonances were difficult to assign in cABC$_{E117C}$ because several peaks in cABC$_{E117C}$ plausibly map to a peak in cABC. To deal with this ambiguity, two putative assignment lists for cABC$_{E117C}$ were produced. The first assumes that the resonance position in cABC$_{E117C}$ is furthest from that in cABC, and the second assumes that the resonance position in cABC$_{E117C}$ is closest to that in the cABC. The chemical-shift perturbation (CSP) values obtained in both cases are essentially identical. In the text, we show the assignment list assuming cABC$_{E117C}$ is furthest from cABC. Here, we show the assignment list assuming cABC$_{E117C}$ is nearest wild type. (*D*) The CSP values when mapped onto the structure of cABC are essentially indistinguishable.

1. Petrova T, et al. (2010) X-ray-induced deterioration of disulfide bridges at atomic resolution. *Acta Crystallogr D Biol Crystallogr* 66(Pt 10):1075–1091.

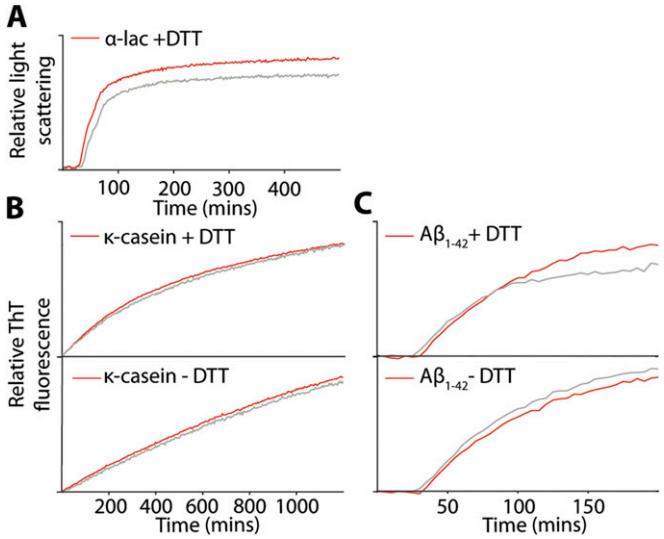

Fig. S3. Chaperone activity of cHSP27, equivalent to data presented for the ABC constructs in Fig. 5. Aggregation traces without chaperone are shown in red, and those with chaperone are shown in gray. cHSP27 is ineffective in protecting against the aggregation of (*A*) α-lactalbumin (α-lac), (*B*) κ-casein, and (*C*) $A\beta_{1–42}$. Molar ratios are the same as in the cABC experiments (main text).

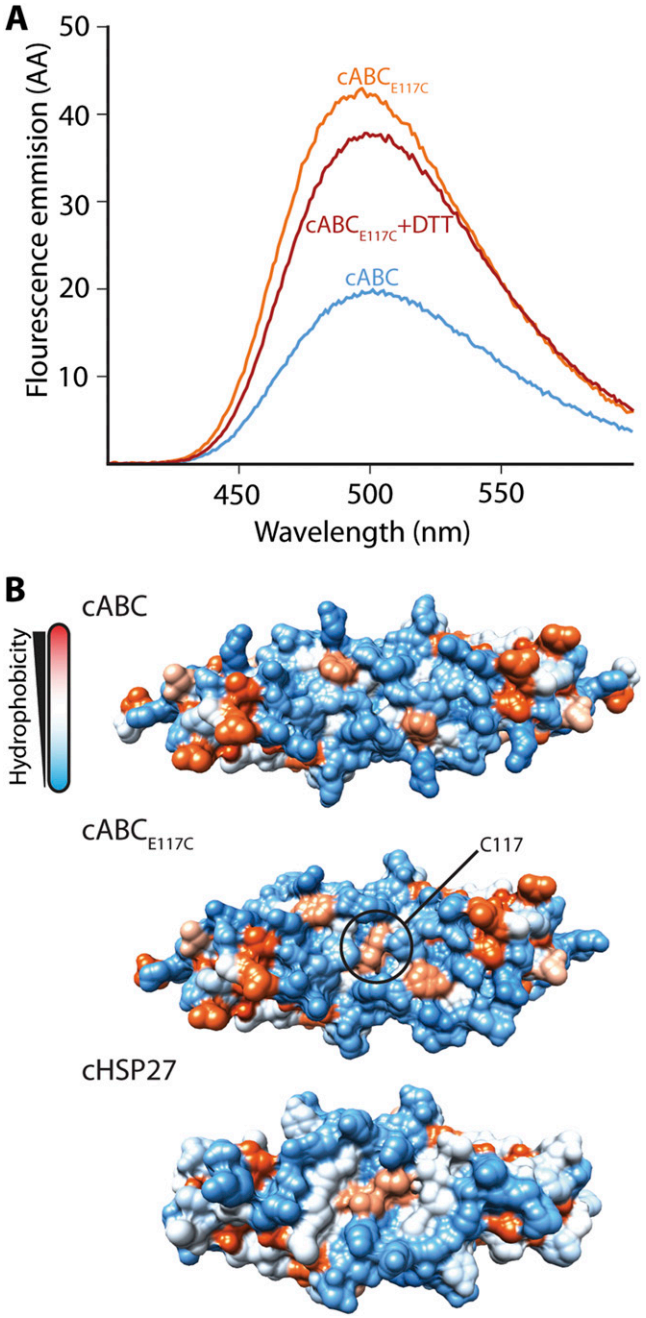

Fig. S4. Mutating E117 in cABC to a cysteine increases the exposed hydrophobic surface area of cABC$_{E117C}$. (*A*) bis-ANS (4,4′-dianilino-1,1′-binaphthyl-5,5′-disulfonic acid) binding to core domain forms of ABC reveals that cABC$_{E117C}$ displays higher bis-ANS fluorescence than cABC under both oxidizing and reducing conditions, suggesting an increased exposed hydrophobic surface in cABC$_{E117C}$. (*B*) Molecular surface of cABC, cABC$_{E117C}$, and cHSP27 colored according to Kyte–Doolittle hydrophobicity (1).

1. Kyte J, Doolittle RF (1982) A simple method for displaying the hydropathic character of a protein. *J Mol Biol* 157(1):105–132.

Table S1. Statistics of X-ray data collection and refinement for cABC, $cABC_{E117C}$, and cHSP27

	cABC	$cABC_{E117C}$	cHSP27
Crystal parameters			
Space group	I222	C2	$P2_1$
Cell dimensions			
a, b, c, Å	35.38, 47.86, 122.84	117.01, 46.77, 77.71	31.28, 48.96, 57.54
α, β, γ, degrees	90, 90, 90	90, 90, 90	90, 99.95, 90
Molecules in A.U.	2	8	4
Data collection			
Synchrotron beamline	APS (24-ID-C)	APS (24-ID-E)	In-house* (DSE-1.2)
Wavelength, Å	0.979	0.979	1.542
Resolution, Å	19.6–1.37	69–2.0	37–2.6
Reflections observed/unique	167,150/21,884	87,187/25,505	38,626/5,331
Completeness, %	97.5 (96.0) †	97.6 (97.52)	99.0 (89.5)
$R_{mrgd\text{-}F}$, %	4.5 (54.6)	6.9 (43.4)	7.8 (53.7)
I/σI	25.13 (3.33)	14.10 (3.5)	17.21 (3.2)
Refinement			
Resolution, Å	19.57–1.37	68.8–2.0	37–2.6
R_{work}, %§	15.6 (17.4)	19.3 (25.3)	23.4 (27.7)
R_{free}, %¶	18.8 (23.9)	24.4 (31.9)	26.6 (34.9)
No. of non-H atoms			
Protein	823	2993	1,397
Nonprotein	79	117	1
Avg. B-factors	24.2	40.1	50.5
Rmsd			
Bond length, Å	0.016	0.008	0.012
Bond angle, degrees	1.64	1.24	0.995
Registration state‖	AP_{III}	AP_{II}	AP_{II}
PDB ID code	4M5S	4M5T	4MJH

A.U., asymmetric unit.

*Data were collected using an FRD rotating anode generator with R-AXIS HTC imaging plate detector.

†Values in parentheses correspond to the highest-resolution shell.

‡$R_{mrgd\text{-}F} = (\Sigma|AI(h,P) - AI(h,Q)|)/(0.5* \Sigma\ AI(h,P) + AI(h,Q))$ where $AI = (\sqrt{I}$ if $I \geq 0$ or $-\sqrt{I}$ if $I < 0)$ as described previously (1).

§$R_{work} = \Sigma \mid F_o - F_c \mid / \Sigma\ F_o$.

¶R_{free} calculated using 5% of the data.

‖Registration state nomenclature as delineated previously (2).

1. Kabsch W (1993) Automatic processing of rotation diffraction data from crystals of initially unknown symmetry and cell constants. *J Appl Cryst* 26(6):795–800.
2. Laganowsky A, et al. (2010) Crystal structures of truncated alphaA and alphaB crystallins reveal structural mechanisms of polydispersity important for eye lens function. *Protein Sci* 19(5): 1031–1043.